CHEMISTRY
A EUROPEAN JOURNAL

ChemPubSoc
Europe

DOI: 10.1002/chem.201203517

# Diels–Alder and Retro-Diels–Alder Cycloadditions of (1,2,3,4,5-Pentamethyl)cyclopentadiene to La@$C_{2v}$-$C_{82}$: Regioselectivity and Product Stability

**Marc Garcia-Borràs,[a] Josep M. Luis,*[a] Marcel Swart,*[a, b] and Miquel Solà*[a]**

**Abstract:** One of the most important reactions in fullerene chemistry is the Diels–Alder (DA) reaction. In two previous experimental studies, the DA cycloaddition reactions of cyclopentadiene (Cp) and 1,2,3,4,5-pentamethylcyclopentadiene (Cp*) with La@$C_{2v}$-$C_{82}$ were investigated. The attack of Cp was proposed to occur on bond **19**, whereas that of Cp* was confirmed by X-ray analysis to be over bond **o**. Moreover, the stabilities of the Cp and Cp* adducts were found to be significantly different, that is, the decomposition of La@$C_{2v}$-$C_{82}$Cp was one order of magnitude faster than that of La@$C_{2v}$-$C_{82}$Cp*. Herein, we computationally analyze these DA cycloadditions with two main goals: First, to compute the thermodynamics and kinetics of the cycloadditions of Cp and Cp* to different bonds of La@$C_{2v}$-$C_{82}$ to assess and compare the regioselectivity of these two reactions. Second, to understand the origin of the different thermal stabilities of the La@$C_{82}$Cp and La@$C_{82}$Cp* adducts. Our results show that the regioselectivity of the two DA cycloadditions is the same, with preferred attack on bond **o**. This result corrects the previous assumption of the regioselectivity of the Cp attack that was made based only on the shape of the La@$C_{82}$ singly occupied molecular orbital. In addition, we show that the higher stability of the La@$C_{82}$Cp* adduct is not due to the electronic effects of the methyl groups on the Cp ring, as previously suggested, but to higher long-range dispersion interactions in the Cp* case, which enhance the stabilization of the reactant complex, transition state, and products with respect to the separated reactants. This stabilization for the La@$C_{82}$Cp* case decreases the Gibbs reaction energy, thus allowing competition between the direct and retro reactions and making dissociation more difficult.

**Keywords:** cycloaddition · Diels–Alder reaction · fullerenes · lanthanum · regioselectivity

## Introduction

Since the discovery of La@$C_{60}$ by Smalley, Kroto, and co-workers in 1985,[1] endohedral metallofullerenes (EMFs) have received continuous growing interest because of their potential applications in a variety of fields, ranging from molecular electronics to biomedical uses.[2] Six years after the detection of La@$C_{60}$, Smalley and co-workers published the formation of macroscopic quantities of higher fullerenes with La inside, including La@$C_{82}$.[3] Nowadays, among the different types of available EMFs,[4] M@$C_{82}$ (M = Group 2 or 3 metal) are the most abundant.[5] Many of the rare-earth elements have been encapsulated within $C_{82}$ cages to form not only M@$C_{82}$ but also $M_2$@$C_{82}$, $M_2C_2$@$C_{82}$, and $MS_2$@$C_{82}$ EMFs. Interestingly, depending of the nature of the encapsulated cluster, the $C_{82}$ cage can have different symmetries. Thus, among others, the $C_s$-$C_{82}$ cage encapsulates La,[6] $Sc_2C_2$,[7] $Y_2C_2$,[8] $Sc_2(\mu_2\text{-S})$,[9] and $Sc_2(\mu_2\text{-O})$ clusters,[10] the $C_{2v}$-$C_{82}$ cage usually contains a single metal, such as La,[6] Y,[11] Sc,[12] and Ce,[13] although it can also incarcerate $Y_2C_2$,[8] and the $C_{3v}$-$C_{82}$ fullerene encloses $M_2$ (M = Y, Sc),[8a,14] $M_2C_2$ (M = Sc, Y, Dy),[8,14,15] $MS_2$ (M = Sc, Y, Dy, and Lu),[16] and $Sc_2(\mu_2\text{-S})$ metal clusters.[9]

Among the different rare-earth elements that have been encapsulated within $C_{82}$, La@$C_{82}$ has probably been the most studied.[3] It can be found encapsulated in the isolated pentagon rule (IPR) obeying $C_{2v}$-$C_{82}$ and $C_s$-$C_{82}$ cages. Because La@$C_{2v}$-$C_{82}$ is more abundant than La@$C_s$-$C_{82}$, most of the analysis of the electronic and molecular structure, as well as the reactivity, of La@$C_{82}$ species has involved the La@$C_{2v}$-$C_{82}$ EMF. The maximum entropy method (MEM)/Rietveld analysis by using synchrotron powder diffraction revealed that, in La@$C_{2v}$-$C_{82}$, the La atom is located at an off-centered position on the $C_2$ axis, adjacent to a hexagonal ring of the fullerene structure.[17] Because of the location of the La atom, this EMF has 24 non-equivalent C atoms,[2a] 19 different [6,6] bonds, and 16 different [5,6] bonds (Figures 1 and 2). Interestingly, when the temperature is high enough,

[a] M. Garcia-Borràs, Dr. J. M. Luis, Prof. Dr. M. Swart, Prof. Dr. M. Solà
Institut de Química Computacional and
Departament de Química, Universitat de Girona
Campus Montilivi, 17071 Girona, Catalonia (Spain)
E-mail: josepm.luis@udg.edu
marcel.swart@icrea.cat
miquel.sola@udg.edu

[b] Prof. Dr. M. Swart
Institució Catalana de Recerca i Estudis Avançats (ICREA)
Pg. Lluís Companys 23, 08010 Barcelona, Catalonia (Spain)

Supporting information for this article is available on the WWW under http://dx.doi.org/10.1002/chem.201203517.

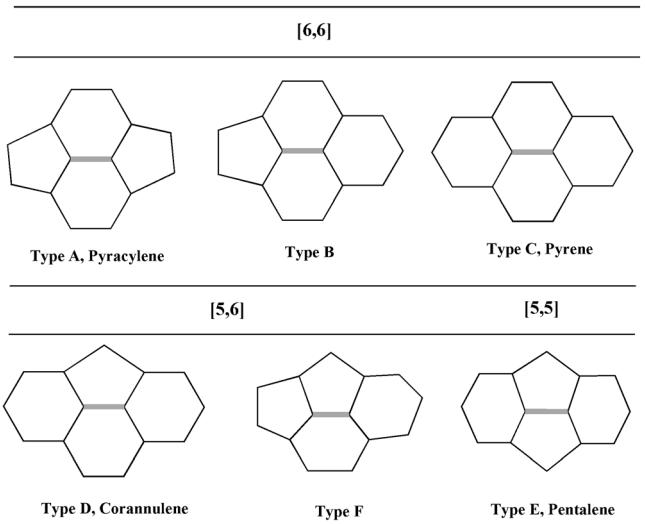


Figure 1. Representation of the different [6,6], [5,6], and [5,5] bond types that are more commonly found in fullerene structures.

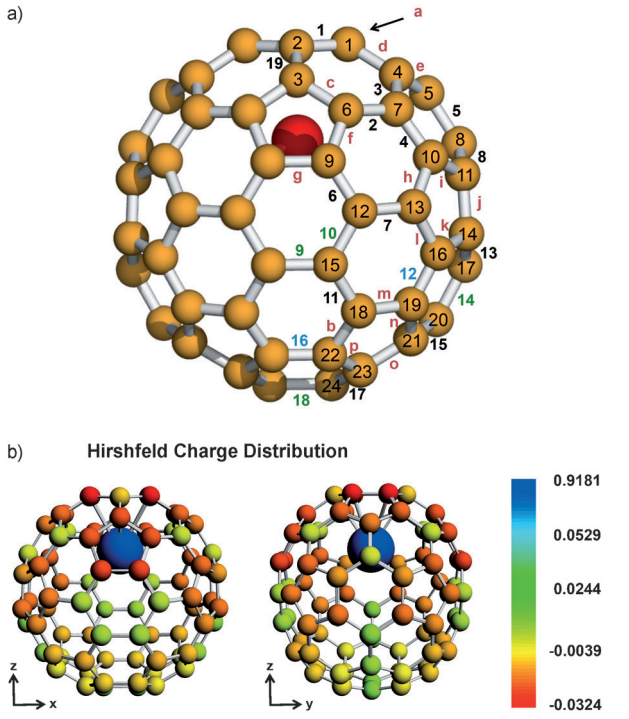


Figure 2. a) Representation of the different non-equivalent bonds of La@$C_{2v}$-$C_{82}$; numbers denote [6,6] bonds and lower-case letters denote [5,6] bonds. Different colors are used to label the different bond types (Figure 1; type A: blue, type B: black, type C: green; type D: red). To facilitate comparison, we kept the same atom numbering as in previous studies.[23,30] b) Atomic Hirshfeld charge distribution of La@$C_{2v}$-$C_{82}$ at the BLYP-$D_2$/TZP//BLYP-$D_2$/DZP level of theory.

the La atom can undergo a boat-shape movement around the equilibrium position.[18]

In the ionic model, the formal electronic structure of La@$C_{2v}$-$C_{82}$ is described as $La^{3+}$@$C_{2v}$-$C_{82}^{3-}$,[19] in which the fullerene cage contains an unpaired number of electrons (for the molecular-orbital diagram of La@$C_{2v}$-$C_{82}$, see the Supporting Information). The paramagnetic nature of this EMF impedes its direct NMR determination[20] and makes La@$C_{2v}$-$C_{82}^{-}$ an unusually stable metallofullerene anion.[21] As expected from symmetry arguments, the $^{13}$C NMR spectrum of La@$C_{2v}$-$C_{82}^{-}$ exhibits 24 distinct lines (17 of almost-equal intensity and seven of half intensity),[21] thus confirming the presence of 24 non-equivalent C atoms. With regards to the redox properties and because of its radical character, La@$C_{2v}$-$C_{82}$ is a stronger electron donor and electron acceptor than empty $C_{2v}$-$C_{82}$.[22] This type of amphoteric compounds, that is, systems with high electron affinity and low ionization potential, are very interesting in the field of molecular electronics. Moreover, the reversible gain or loss of electrons in La@$C_{82}$ are useful for controlling its reactivity towards nucleophiles and electrophiles.[22]

The reactivity of La@$C_{2v}$-$C_{82}$ has been analyzed in a number of studies. Because of its low-energy singly occupied molecular orbital (SOMO), La@$C_{2v}$-$C_{82}$ is expected to react faster than $C_{60}$.[23] The first derivatization of an EMF involved the photochemical addition of a disilirane to La@$C_{82}$.[19b] Other similar additions to La@$C_{82}$ include the photochemical addition of digermirane,[24] the Bingel addition,[25] the cycloadditions of diphenyldiazomethane[26] and 5,10,15,20-tetraphenylporphyrin,[27] as well as the addition of adamantylidene that was generated from 2-adamantane-2,3-[3*H*]-diazirine, which occurred on the [6,6] bond **1** (Figure 2a) in what was the first example of a selective reaction on La@$C_{2v}$-$C_{82}$.[20,28] Very recently, Akasaka, Lu, and co-workers reported that the reaction of M@$C_{2v}$-$C_{82}$ (M = Y, La, Ce, Gd) with diazirine adamantylidene only produced two monoadduct isomers, whereas the reaction for M = Sc produced four regioisomers.[29] Another group of reactions of La@$C_{2v}$-$C_{82}$ corresponds to radical addition reactions. In this group, we find the addition of the benzyl radical, which comes from the thermal or photochemical decomposition of 3-triphenylmethyl-5-oxazolidinone, on the C10 and C23 carbon atoms of the cage (Figure 2a),[5] the formation of the (La@$C_{2v}$-$C_{82}$)$_2$ dimer from two La@$C_{2v}$-$C_{82}$ units that are connected through a long C–C bond,[25b,30] and the thermal retro-reaction of radical monoadducts in the presence of a radical trapping reagent, such as (2,2,6,6-tetramethylpiperidin-1-yl)oxyl (TEMPO).[31] Finally, in a very recent publication, the Prato cycloaddition of azomethine ylide, which was generated in situ from *n*-octylglycine and 2-formyl-9,10-bis(1,3-dithiol-2-ylidene)-9,10-dihydroanthracene, to La@$C_{2v}$-$C_{82}$ has been reported to most likely occur on bond **o** (Figure 2a).[32]

One of the most important reactions in fullerene chemistry is the Diels–Alder (DA) reaction,[33] which has also been carried out on La@$C_{2v}$-$C_{82}$. In the DA cycloaddition of cyclopentadiene (Cp),[23] the attack of Cp on bond **19** (Figure 2a) was proposed to yield the major product. It should be mentioned here that the product, La@$C_{2v}$-$C_{82}$Cp, was actually not isolated and that the proposed attack on bond **19** was only made on the basis of the shape of the SOMO. In a later work,[30] 1,2,3,4,5-pentamethylcyclopentadiene (Cp*)

  

was used and X-ray crystallographic analysis indicated that the major product of the DA addition corresponded to the attack on bond **o**. This regioselectivity was later confirmed in the same work for the double addition of Cp* and adamantylidene.[30] The fact that two relatively similar dienes (Cp and Cp*) have markedly different regioselectivities is surprising. Moreover, the stabilities of the Cp and Cp* adducts were also found to be significantly different. Thus, at 298 K, only 36% of La@$C_{82}$Cp* decomposes into La@$C_{82}$ and Cp* after 12 h,[30] whereas the half-life of La@$C_{82}$Cp under the same conditions is only $\tau = 1.8$ h (for comparison, $\tau = 1800$ h for the decomposition of $C_{60}$Cp).[23] This higher stability of the La@$C_{82}$Cp* adduct was attributed to the electronic effects of the methyl groups on the Cp ring.[30] We anticipate that this work will show that this conclusion does not hold.

Herein, we report a theoretical study of the DA cycloaddition reactions between Cp or Cp* and La@$C_{2v}$-$C_{82}$ with two main goals: 1) To compute the thermodynamics and kinetics of the cycloadditions of Cp and Cp* to different bonds of La@$C_{2v}$-$C_{82}$ to assess and compare the regioselectivity of these two reactions and 2) to understand the origin of the different thermal stabilities of the La@$C_{82}$Cp and La@$C_{82}$Cp* adducts. This theoretical study represents another step forward towards a detailed understanding of the changes in chemical reactivity owing to the incarceration of atoms or clusters of atoms, which is essential for assisting the synthesis of new functionalized endohedral fullerenes with specific properties.[34]

## Computational Details

All density functional theory (DFT) calculations were performed by using the Amsterdam density functional (ADF) program.[35] The molecular orbitals (MOs) were expanded in an uncontracted set of Slater-type orbitals (STOs) of double-ζ (DZP) and triple-ζ (TZP) quality that contained diffuse functions and one set of polarization functions. To shorten the computational time that was needed to carry out the calculations, the frozen-core approximation was used.[36] In this approximation, the core density is obtained and included explicitly, albeit with core orbitals (1s for C and 1s2s2p3s3p4s3d4p for La) that are kept frozen during the SCF procedure. It has been shown that the frozen-core approximation has a negligible effect on the optimized equilibrium geometries.[37] Scalar relativistic corrections have been included self-consistently by using the zeroth order regular approximation (ZORA).[38] An auxiliary set of s, p, d, f, and g STOs was used to fit the molecular density and to accurately represent the Coulomb and exchange potentials for each SCF cycle.[39] Energies and gradients were calculated by using the local density approximation (Slater exchange) with non-local corrections for exchange (Becke88)[40] and correlation (Lee–Yang–Parr)[41] included self-consistently (i.e., the BLYP functional). Open-shell systems were treated with the unrestricted formalism (UBLYP or UB3LYP). Moreover, energy-dispersion corrections were introduced by using the Grimme methodology[42] ($D_2$), as implemented in ADF version 2010.01.[35] All of the structures were fully optimized by using these corrections in each optimization step. It has been shown that dispersion corrections are essential for a correct description of the thermodynamics and kinetics of the reactions of fullerenes and nanotubes.[43] Our results are not corrected for the basis set superposition error (BSSE). By using the Boys and Bernardi counterpoise method to correct the BSSE,[44] we found that the BSSE correction only destabilized the van der Waals intermediate in the attack of Cp on the **o** bond of $C_{82}$ with respect to the separated reactants by 1.05 kcal mol$^{-1}$ at the B3LYP-$D_2$/TZP//BLYP-$D_2$/DZP level. Because all van der Waals intermediates have similar fullerene–diene separations, we expect about the same small destabilization for all intermediates. Consequently, we expect that BSSE will not modify the main conclusions of this work.

All of the energies reported herein were obtained with the TZP basis in single-point energy calculations at geometries that were optimized with the DZP basis (i.e., BLYP-$D_2$/TZP//BLYP-$D_2$/DZP). It is well-documented that standard DFT functionals, such as BLYP-$D_2$, underestimate energy barriers.[45] Nevertheless, in previous work,[43a,46] it has been shown that the B3LYP functional gives accurate results for the barriers in Diels–Alder reactions involving fullerene species when dispersion corrections ($D_2$) are included (B3LYP-$D_2$). Thus, to validate and complement our results, we performed single-point energy calculations for the most favored additions of Cp and Cp* on La@$C_{82}$ at the B3LYP-$D_2$/TZP level of theory[41,47] (i.e., B3LYP-$D_2$/TZP//BLYP-$D_2$/DZP; for further discussion, see below and the Supporting Information). We did not perform the whole study at the B3LYP-$D_2$ level owing to the high computational cost of these calculations when using a hybrid functional in the ADF program. On the contrary, this program is very efficient for computationally demanding studies, such as this one, when a GGA functional is used because of the good parallelization of this program. Moreover, we already anticipate here that, although BLYP-$D_2$ underestimates the absolute values of the reaction barriers, the trend for the reactivity of the different bonds is not affected.

The actual geometry optimizations and transition-state (TS) searches were performed by using the QUILD (quantum regions interconnected by local descriptions) program,[48] which functions as a wrapper around the ADF program. The QUILD program constructs the input files for the ADF, runs the ADF, and collects the data; the ADF is used only for the generation of the energy and the gradients. Furthermore, the QUILD program uses improved geometry-optimization techniques, such as adapted delocalized coordinates[49] and specially constructed model Hessians with the appropriate number of eigenvalues.[49] This latter technique is particularly useful for TS searches. All TSs were characterized by computing the analytical[50] vibrational frequencies, to have only one imaginary frequency, which corresponds to the approach of the reacting carbon atoms. In selected DA attacks, analytical Hessians were computed for all of the stationary points along the reaction coordinated to calculate unscaled zero-point energies (ZPEs), as well as thermal corrections and entropy effects, by using the standard statistical-mechanics relationships for an ideal gas.[51] These latter two terms were computed at 298.15 K and 1 atm to provide the reported relative Gibbs energies ($\Delta G_{298}$). The reported Gibbs energies were obtained from the electronic energies that were computed at the BLYP-$D_2$/TZP//BLYP-$D_2$/DZP or B3LYP-$D_2$/TZP//BLYP-$D_2$/DZP levels of theory, corrected by the ZPEs and thermal and entropy terms calculated by using the BLYP-$D_2$/DZP method.

Pyramidalization angles, first introduced by Haddon[52] as a measure of the local curvature in polycyclic aromatic hydrocarbons, were calculated by using the POAV3 program.[53]

## Results and Discussion

In this section, we discuss the thermodynamics of the DA cycloadditions of cyclopentadiene on all of the different bonds of the La@$C_{2v}$-$C_{82}$ EMF. The kinetics of the most exothermic additions are also analyzed. Moreover, for the most reactive bonds, we also discuss the thermodynamics and kinetics of the DA addition of Cp* to La@$C_{2v}$-$C_{82}$. Finally, we explain the different behavior and stability of the two final most stable products by analyzing their retro-DA reactions.

**Molecular and electronic structures of La@$C_{2v}$-$C_{82}$, cyclopentadiene, and 1,2,3,4,5-pentamethylcyclopentadiene**: As

  

explained in the Introduction, the formal charge transfer from the metallic atom to the fullerene cage is of three electrons, thus giving a formal $La^{+3}@C_{82}^{-3}$ ionic structure. The BLYP-$D_2$/TZP//BLYP-$D_2$/DZP results indicate that the charge on the La atom in the EMF structure is 0.63/0.92 (Voronoi/Hirshfeld, Figure 2b). Not surprisingly, this charge is much less than the expected formal charge from the ionic model.

An interesting analysis can be performed from the frontier molecular orbitals (MOs) of the different species involved. Because the La@$C_{2v}$-$C_{82}$ EMF is our present dienophile, we have to pay attention to its SOMO, which will interact with the HOMO of the diene (Cp or Cp*) during the DA addition. We are studying a concerted cycloaddition reaction in which there is a movement of two electrons from the HOMO of the diene onto the dienophile. Thus, a reaction that involves the partially occupied SOMO of the EMF, which can only host one of the transferred electrons, is forced to gain support from other unoccupied MOs, in which this extra electron can be placed. This result means that we have to also consider at least the LUMO of the EMF species to correctly describe the electronic rearrangement during the reaction. These SOMO and LUMO of La@$C_{2v}$-$C_{82}$ are very close in energy to the HOMOs of Cp and Cp* (Figure 3a). In the case of Cp (Cp*), the $HOMO_{diene}$–$SOMO_{EMF}$ gap is 0.13 eV (−0.77 eV) and the $HOMO_{diene}$–$LUMO_{EMF}$ gap is 0.72 eV (−0.15 eV). Although previous studies[23,30] only took into account the SOMO when analyzing the interactions between the Cp/Cp* and the EMF during the DA reaction, herein we have extended the analysis to the LUMO. This choice is justified by the electronic characteristics of the reaction and by the small HOMO–SOMO and HOMO–LUMO gaps.

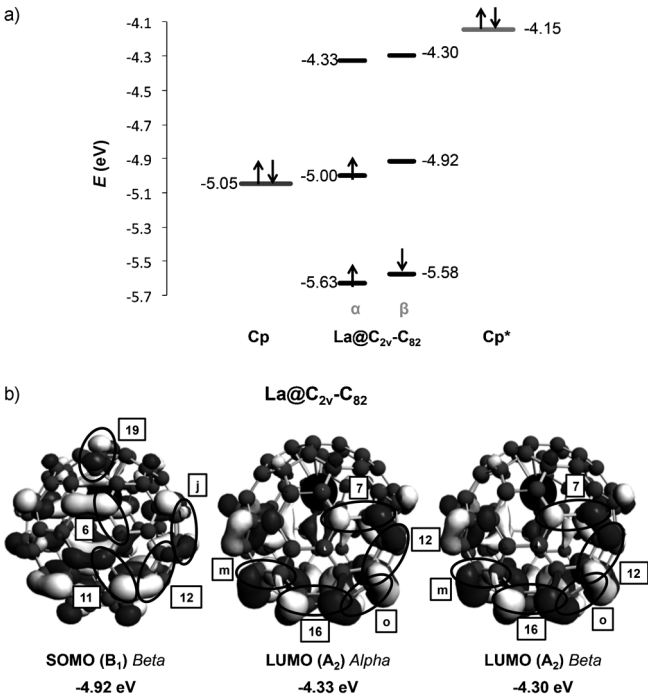


Figure 3. a) Molecular-orbital levels of the frontier orbitals of La@$C_{82}$, cyclopentadiene (Cp), and 1,2,3,4,5-pentamethylcyclopentadiene (Cp*). b) Representation of the SOMO (unoccupied *beta*) and LUMOs (*alpha* and *beta*) of La@$C_{2v}$-$C_{82}$ (isosurface value: 0.02); only those bonds with favorable orbitals for interactions with the HOMO of the diene are marked with ellipses. Energy values of the levels are given in eV.

In Figure 3b, the SOMO and LUMO of the La@$C_{2v}$-$C_{82}$ EMF are represented. This figure shows that bonds **6**, **11**, **12**, **19**, and **j** all have the correct shape in the SOMO (with antibonding lobes in the attacked bond) to interact with the HOMO of the diene. In the LUMO, the bonds with the correct shape are **7**, **12**, **16**, **m**, and **o**. From these initial observations, we can conclude that bond **12**, which has the correct shape in both cases, could be the most favorable addition site.

The LUMO lobes are mainly located in the lower half of the La@$C_{2v}$-$C_{82}$ molecule, far away from the La atom, which is located in the upper half. By considering the charge distribution in the entire molecule, as represented in Figure 2b, we can see that the upper half is closest to the lanthanum atom and, more specifically, that the five-membered rings (5-MRs) accumulate the main part of the negative charge, as expected.[54] This concentration of negative charge on the 5-MRs that are placed nearest to the metallic atom prompts the non-uniform shape of the LUMO.

From the geometric parameters, we can extract several conclusions. Table 1 lists all the non-equivalent bonds lengths and pyramidalization angles. These latter values were calculated as the average of the two atoms that were involved in the attacked bond. As expected, [6,6] bonds have, in general, shorter bond lengths and smaller pyramidalization angles than [5,6] bonds (see the average values in Table 1). We must remind the reader that high pyramidalization angles and shorter C–C separation usually favor the cycloaddition reactions.[55] Therefore, bonds **12** and **16**, which are [6,6] bonds with shorter bond lengths and the highest pyramidalization angles are initially good candidates to be among the most reactive bonds. We also have to consider bonds **1** and **19**, which have high pyramidalization angles, and bonds **4**, **8**, and **17**, which have short C–C separation. On the other hand, for the [5,6] bonds, we can see that the bond lengths all fall within a very small range (between 1.430 and 1.463 Å) and that only two bonds (**f** and **g**) have pyramidalization angles narrower than 10° (the range of the pyramidalization angles is also quite small, from 9.64 to 10.81°). Because [5,6] bonds have relatively similar bond lengths and pyramidalization angles, it is difficult to use these criteria to suggest which of them could be the most reactive based only on the geometric parameters.

Taking into account the shapes of the SOMO and LUMO and the geometric parameters, we expect [6,6] bonds **12**, **16**, and **19** and [5,6] bonds **j**, **m**, and **o** to be the most reactive. As mentioned in the Introduction, the preferential attack of Cp has been suggested to occur on bond **19** (without any convincing evidence, such as a crystal structure),[23] whereas the preferential attack of Cp* has been suggested to occur on bond **o**.[30] Both bonds **19** and **o** are among the initial candidates to be the most reactive bond.

  

Table 1. BLYP-$D_2$/TZP//BLYP-$D_2$/DZP reaction energies ($\Delta E_R$) for the Diels–Alder cycloaddition of cyclopentadiene over all non-equivalent bonds of the La@$C_{2v}$-$C_{82}$ EMF. Bond lengths ($R_{full}$) and pyramidalization angles ($\theta_p$) for free La@$C_{2v}$-$C_{82}$, and the bond lengths of the C–C bonds over which the reaction took place and of the two new C–C bonds ($R_{CC}$) in the products are also presented.

| | | La@$C_{2v}$-$C_{82}$ | | La@$C_{2v}$-$C_{82}$Cp | | | |
|---|---|---|---|---|---|---|---|
| Product | Bond type | $R_{full}$ [Å] | $\theta_p$ [a] [°] | $\Delta E_R$ [kcal mol$^{-1}$] | $R_{full}$ [Å] | $R_{CC}$ [Å] | |
| **1** | B [6,6] | 1.448 | 10.54[b] | −2.1 | 1.641 | 1.595 | 1.615 |
| **2** | B [6,6] | 1.424 | 9.51 | 4.9 | 1.630 | 1.607 | 1.616 |
| **3** | B [6,6] | 1.441 | 9.63 | 8.2 | 1.644 | 1.604 | 1.615 |
| **4** | B [6,6] | 1.415[b] | 9.68 | −3.1 | 1.625 | 1.599 | 1.609 |
| **5** | B [6,6] | 1.439 | 9.32 | 15.3 | 1.643 | 1.613 | 1.624 |
| **6** | B [6,6] | 1.424 | 8.74 | 8.4 | 1.607 | 1.623 | 1.624 |
| **7** | B [6,6] | 1.425 | 9.33 | −0.2 | 1.648 | 1.609 | 1.619 |
| **8** | B [6,6] | 1.422[b] | 9.68 | 3.8 | 1.626 | 1.607 | 1.621 |
| **9** | C [6,6] | 1.468 | 7.55 | 15.3 | 1.690 | 1.618 | 1.618 |
| **10** | C [6,6] | 1.465 | 7.69 | 16.3 | 1.697 | 1.613 | 1.616 |
| **11** | B [6,6] | 1.425 | 9.25 | −4.6[b] | 1.659 | 1.603 | 1.619 |
| **12** | A [6,6] | 1.380[b] | 10.73[b] | −5.5[b] | 1.554 | 1.614 | 1.620 |
| **13** | B [6,6] | 1.426 | 9.70 | 0.7 | 1.640 | 1.604 | 1.617 |
| **14** | C [6,6] | 1.471 | 9.58 | 16.4 | 1.730 | 1.613 | 1.616 |
| **15** | B [6,6] | 1.427 | 9.51 | 1.9 | 1.642 | 1.605 | 1.624 |
| **16** | A [6,6] | 1.374[b] | 10.67[b] | −6.4[b] | 1.553 | 1.613 | 1.613 |
| **17** | B [6,6] | 1.422[b] | 9.60 | −0.2 | 1.634 | 1.601 | 1.622 |
| **18** | C [6,6] | 1.475 | 8.55 | 20.7 | 1.736 | 1.619 | 1.619 |
| **19** | B [6,6] | 1.434 | 10.27[b] | −5.1[b] | 1.646 | 1.599 | 1.614 |
| **a** | D [5,6] | 1.463 | 10.79[b] | 5.3 | 1.691 | 1.601 | 1.601 |
| **b** | D [5,6] | 1.437 | 10.81[b] | 1.7 | 1.610 | 1.611 | 1.617 |
| **c** | D [5,6] | 1.448 | 10.20 | 0.5 | 1.633 | 1.601 | 1.608 |
| **d** | D [5,6] | 1.448 | 10.60 | −6.2[b] | 1.641 | 1.593 | 1.599 |
| **e** | D [5,6] | 1.434[b] | 10.09 | −4.9[b] | 1.636 | 1.595 | 1.603 |
| **f** | D [5,6] | 1.432[b] | 9.90 | −5.3[b] | 1.643 | 1.600 | 1.607 |
| **g** | D [5,6] | 1.432[b] | 9.64 | 4.0 | 1.596 | 1.610 | 1.610 |
| **h** | D [5,6] | 1.439 | 10.66 | −4.0[b] | 1.630 | 1.606 | 1.610 |
| **i** | D [5,6] | 1.451 | 10.49 | 0.7 | 1.627 | 1.612 | 1.612 |
| **j** | D [5,6] | 1.432[b] | 10.70 | −7.1[b] | 1.630 | 1.604 | 1.605 |
| **k** | D [5,6] | 1.442 | 10.77[b] | 6.0 | 1.606 | 1.610 | 1.624 |
| **l** | D [5,6] | 1.437 | 10.73 | 5.3 | 1.617 | 1.600 | 1.607 |
| **m** | D [5,6] | 1.439 | 10.88[b] | 1.1 | 1.613 | 1.596 | 1.614 |
| **n** | D [5,6] | 1.450 | 10.63 | 4.5 | 1.617 | 1.614 | 1.620 |
| **o** | D [5,6] | 1.430[b] | 10.55 | −10.5[b] | 1.631 | 1.600 | 1.601 |
| **p** | D [5,6] | 1.452 | 10.66 | 6.4 | 1.616 | 1.598 | 1.615 |
| average | [6,6] | 1.430 | 9.47 | 3.54 | 1.640 | 1.608 | 1.618 |
| | [5,6] | 1.441 | 10.49 | −0.23 | 1.625 | 1.603 | 1.610 |

[a] Average values from the two C atoms involved; the values were calculated by taking into account the total number of bonds present in the entire fullerene structure. [b] The expected most-favored bonds from each geometric parameter for the [6,6] and [5,6] bond types (in La@$C_{2v}$-$C_{82}$) and the most reactive bonds under thermodynamic control.

**Reaction energies and energy barriers for the Diels–Alder cycloaddition reactions of cyclopentadiene and 1,2,3,4,5-pentamethylcyclopentadiene with the La@$C_{2v}$-$C_{82}$ EMF**: *Thermodynamics of the Diels–Alder reactions.* The reaction energies that were obtained at the BLYP-$D_2$/TZP//BLYP-$D_2$/DZP level of theory for the DA addition of cyclopentadiene over all 35 non-equivalent bonds of La@$C_{2v}$-$C_{82}$ are listed in Table 1. It is important to note that the reaction energies listed in Table 1 are relative energies with respect to infinitely separated Cp and La@$C_{2v}$-$C_{82}$. For each attack on a [5,6] bond, there are two possible intermediates and two possible products, depending whether the approaching Cp ring faces the 6-MR or the 5-MR of the fullerene. The additions reported in this work correspond to the Cp or Cp* rings that face the 6-MR of the attacked [5,6] bonds. For the attack on [5,6] bond **o**, we have found that the differences between the intermediates and the products of the two attacks are less than 0.5 kcal mol$^{-1}$. For the [6,6] bonds, in some cases, the two additions are the same by symmetry or the differences between the two attacks are expected to be even smaller than 0.5 kcal mol$^{-1}$.

As mentioned in the Computational Details section, we have also carried out calculations at the B3LYP-$D_2$/TZP//BLYP-$D_2$/DZP level of theory to check the reliability of our conclusions that were based on the BLYP-$D_2$ calculations, as well as to obtain more-accurate data for the most favored reactions. The results are shown in the Supporting Information, Table S1 and Figure S2.

As can be seen, this reaction is not very exothermic; in general, [5,6] bonds are more exothermic than [6,6] bonds (see average values, Table 1). The most favored thermodynamic product is obtained from the addition on [5,6] bond **o** ($\Delta E_R = -10.5$ kcal mol$^{-1}$ and $\Delta E_R = -15.1$ kcal mol$^{-1}$ at the BLYP-$D_2$ and B3LYP-$D_2$ levels of theory, respectively). We must also remember that bond **o** has a short C–C distance, a high pyramidalization angle (because it is a [5,6]-type bond), and correct shape and energy of the LUMO to interact with the HOMO of the diene.

Therefore, the 10 most reactive bonds are: **o** > **j** ≈ **16** > **d** > **12** > **f** > **19** > **e** > **11** > **h** (Table 1 and the Supporting Information, Table S1). The shapes of the SOMO and LUMO are suitable for interacting with the [6,6] bonds (**16**, **12**, **19**, and **11**) during the DA reaction and, moreover, are favorable from the points of view of bond length and pyramidalization angle. Bonds **12** and **16** are the most favored by these geometric parameters. Bond **19** also has a high pyramidalization angle and makes suitable contributions to the SOMO. Finally, although bond **11** does not have an especially large pyramidalization angle, it presents favorable SOMO contributions and short C–C distances, thus making it appropriate for reaction during the DA cycloaddition reaction.

The scenario is a bit different in the case of the [5,6] bond type. As we have seen in the previous subsection, the differences in the pyramidalization angles and C–C distances were small and it was difficult to make a prediction from these observations alone. From the point of view of the frontier MOs, there are only three [5,6] bonds with the optimal characteristics, that is, bonds **o**, **j**, and **m**. Our results show that bonds **o** and **j** are the two most reactive of all 35 of the non-equivalent bonds that are present in La@$C_{2v}$-$C_{82}$. From the bond lengths in Table 1, we can see that the lengths of C–C bonds **o** and **j** are among the shortest. Bond **m** has the largest pyramidalization angle, together with optimal contributions to the LUMO+1. However, the reaction

  

energy for the attack on this bond is endothermic, thus showing that the formation of product **m** is thermodynamically unfavorable. This result is another example that points out that the geometrical parameters and the LUMOs shapes are not always good indicators of the reactivity of EMFs.[34,43b,56]

Having determined the reaction energies for the additions over all non-equivalent bonds, in Table 2, we present the reaction energies and thermodynamic data for the 10 most favorable cases, in which the formation of the first initial van der Waals complex is taken into account. The formation of the reactant complex implies an energetic stabilization of about $\Delta E = 5.4$–$7.0$ kcal mol$^{-1}$. If we consider the obtained $\Delta E_R$ (int.) energies, we can see that only three of the selected additions remain exothermic. The thermodynamic regioselectivity of the reaction is still well-determined, thus pointing to product **o** as the major and most favored one with a reaction energy and Gibbs reaction energy of $-4.7$ kcal mol$^{-1}$ and $-1.5$ kcal mol$^{-1}$ ($-11.6$ kcal mol$^{-1}$ and $-8.3$ kcal mol$^{-1}$ at the B3LYP-$D_2$ level), respectively. Furthermore, we found the addition reactions on bonds **j** and **16** to have a $\Delta E = -1.7$ and $-0.5$ kcal mol$^{-1}$ ($\Delta G_R$ (int.) = 1.7 and 2.5 kcal mol$^{-1}$), respectively. Our thermodynamic results show that the attack on bond **19** is largely endergonic ($\Delta G_R$ (int.) = 7.1 kcal mol$^{-1}$) and, consequently, we can exclude it as the source of the main adduct product.

By analyzing the formation of La@$C_{2v}$-$C_{82}$Cp, one important observation is that the addition on bond **o** has a favorable reaction Gibbs energy, but only when compared to the initial reactant complex. For all of the addition reactions studied, the reaction entropic term from infinitely separated reactants makes a large contribution to the reaction, which, in all cases, is higher than the contribution of the reaction enthalpy term, thus making the final Gibbs energies (with respect to the reactants) positive. In general, the reaction entropy is practically constant for all non-equivalent additions (between $-50.9$ and $-52.2$ cal mol$^{-1}$K$^{-1}$). Thus, the final regioselectivity of the process is governed by the reaction enthalpy. It is worth noting here that an evaluation of the entropies of the chemical reactions in solution is a challenge to computational chemists. Entropy changes in solution for a bimolecular reaction are usually smaller than in the gas phase. Therefore, by using the gas-phase entropies, as we do herein, the entropic contribution to the reaction Gibbs energies values is likely to be overestimated.[57]

For the four most favored addition sites, that is, bonds **o**, **j**, **16**, and **11**, we have also analyzed their reactions with 1,2,3,4,5-pentamethylcyclopentadiene. The major product

Table 2. BLYP-$D_2$/TZP//BLYP-$D_2$/DZP reaction energies ($\Delta E_R$) and Gibbs reaction energies, enthalpies, and entropies ($\Delta G_R$, $\Delta H_R$, and $\Delta S_R$) for the Diels–Alder cycloaddition reactions of cyclopentadiene and 1,2,3,4,5-pentamethylcyclopentadiene at the most favorable addition sites of the La@$C_{2v}$-$C_{82}$ EMF at 298.15 K. Bond lengths of the C–C bonds on which the reaction took place ($R_{full}$ (int.) and $R_{full}$ (prod.)) and of the two newly formed C–C bonds ($R_{CC}$ (int.) and $R_{CC}$ (prod.)) in the initial intermediates and in the final products are also presented.[a]

| Product | Bond type | $\Delta E_R$ [kcal mol$^{-1}$] | $\Delta G_R$ [kcal mol$^{-1}$] | $\Delta H_R$ [kcal mol$^{-1}$] | $\Delta S_R$ [cal mol$^{-1}$] | $R_{full}$ (prod.) [Å] | $R_{CC}$ (prod.) [Å] | | $R_{full}$ (int.) [Å] | $R_{CC}$ (int.) [Å] | |
|---|---|---|---|---|---|---|---|---|---|---|---|
| *La@$C_{2v}$-$C_{82}$Cp* | | | | | | | | | | | |
| **11** | B [6,6] | −4.6 | 13.5 | −2.0 | −51.9 | 1.659 | 1.603 | 1.619 | 1.424 | 2.871 | 2.992 |
| | | *1.6* | *5.7* | *4.0* | *−5.9* | | | | | | |
| **12** | A [6,6] | −5.5 | 12.6 | −2.8 | −51.5 | 1.554 | 1.614 | 1.620 | 1.379 | 2.885 | 2.917 |
| | | 0.5 | *3.1* | *3.5* | *1.2* | | | | | | |
| **16** | A [6,6] | −6.4 | 11.8 | −3.6 | −51.6 | 1.553 | 1.613 | 1.613 | 1.375 | 2.906 | 2.906 |
| | | *-0.5* | *2.5* | *2.7* | *0.7* | | | | | | |
| **19** | B [6,6] | −5.1 | 12.7 | −2.5 | −51.0 | 1.646 | 1.599 | 1.614 | 1.434 | 2.920 | 2.922 |
| | | *1.9* | *7.1* | *3.7* | *−11.7* | | | | | | |
| **d** | C [5,6] | −6.2 | 11.7 | −3.6 | −51.3 | 1.641 | 1.593 | 1.599 | 1.446 | 2.930 | 2.996 |
| | | *0.3* | *4.1* | *2.7* | *−4.9* | | | | | | |
| **e** | C [5,6] | −4.9 | 13.2 | −2.3 | −51.9 | 1.636 | 1.595 | 1.603 | 1.434 | 2.946 | 2.981 |
| | | *1.3* | *7.3* | *3.4* | *−13.1* | | | | | | |
| **f** | C [5,6] | −5.3 | 12.9 | −2.7 | −52.2 | 1.643 | 1.600 | 1.607 | 1.429 | 2.945 | 3.063 |
| | | *0.2* | *3.4* | *3.2* | *−0.7* | | | | | | |
| **h** | C [5,6] | −4.0 | 13.7 | −1.5 | −50.9 | 1.630 | 1.606 | 1.610 | 1.435 | 2.959 | 2.938 |
| | | *2.0* | *4.9* | *5.0* | *0.3* | | | | | | |
| **j** | C [5,6] | −7.1 | 10.9 | −4.4 | −51.5 | 1.630 | 1.604 | 1.605 | 1.430 | 2.955 | 2.974 |
| | | *−1.7* | *1.7* | *1.4* | *−1.1* | | | | | | |
| **o** | C [5,6] | −10.5 | 7.8 | −7.6 | −51.8 | 1.631 | 1.600 | 1.601 | 1.429 | 2.939 | 2.968 |
| | | *−4.7* | *−1.5* | *−1.5* | *−0.1* | | | | | | |
| *La@$C_{2v}$-$C_{82}$Cp** | | | | | | | | | | | |
| **11** | B [6,6] | −13.1 | 5.6 | −11.1 | −56.2 | 1.656 | 1.616 | 1.643 | 1.430 | 2.776 | 2.886 |
| | | *1.8* | *7.3* | *2.3* | *−16.7* | | | | | | |
| **16** | A [6,6] | −14.8 | 4.0 | −12.8 | −56.3 | 1.553 | 1.633 | 1.633 | 1.381 | 2.784 | 2.789 |
| | | *−0.8* | *5.1* | *−0.1* | *−17.7* | | | | | | |
| **j** | C [5,6] | −15.5 | 2.9 | −13.6 | −55.3 | 1.625 | 1.618 | 1.620 | 1.435 | 2.852 | 2.855 |
| | | *−1.7* | *3.6* | *−1.1* | *−15.9* | | | | | | |
| **o** | C [5,6] | −19.4 | −0.7 | −17.4 | −55.9 | 1.625 | 1.613 | 1.615 | 1.436 | 2.814 | 2.862 |
| | | *−5.1* | *0.5* | *−4.4* | *−16.6* | | | | | | |

[a] Values in italics were obtained relative to the first reactant complex that was formed.

  

for the DA reaction with Cp* was determined from X-ray crystallography to be addition on bond **o**.[30] The results presented in Table 2 show that the addition to bond **o** is clearly preferred over the additions to bonds **j**, **16**, or **11**. The $\Delta E_R$ and $\Delta G_R$ values for the formation of La@$C_{2v}$-$C_{82}$Cp* indicate the regioselective formation of product **o**, according to the experimental observations. If the initial reactant complex is considered as a reference, that is, $\Delta E_R$ (int.) and $\Delta G_R$ (int.), the conclusion is exactly the same.

If the reactions with Cp and Cp* are analyzed and compared, it is found that the Gibbs reaction energies for the addition of Cp* relative to the infinitely separated reactants are much more exothermic than those found for the addition of Cp. The origin of this large reaction Gibbs energy difference is in the enthalpic contribution, whilst the entropic terms are almost identical.

One can see that computed reaction energies ($\Delta E$) relative to the reactant complex are practically identical for the additions of Cp and Cp* on each bond (−4.7 and −5.1 kcal mol$^{-1}$ on bond **o**, −1.7 kcal mol$^{-1}$ on bond **j**, −0.5 and −0.8 kcal mol$^{-1}$ on bond **16**, and +1.8 and +1.6 kcal mol$^{-1}$ on bond **11**, respectively). These observations indicate that, once the reactant complex is formed, electronic effects, owing to the methyl substituents on the cyclopentadiene ring, have a rather small influence on the reaction energies. However, if we look at the $\Delta E_R$ and $\Delta G_R$ values relative to infinitely separated reactants, those values that correspond to the formation of La@$C_{2v}$-$C_{82}$Cp* are about 9 kcal mol$^{-1}$ ($\Delta E_R$) or 7–8 kcal mol$^{-1}$ ($\Delta G_R$) more favorable than their corresponding values for the formation of La@$C_{2v}$-$C_{82}$Cp. The large effect of methyl substitution on the $\Delta E_R$ and $\Delta G_R$ values is already seen in the formation of the reactant complex and, therefore, has to be attributed to the larger dispersion interactions that are operative in Cp* as compared to Cp (see below). Finally, the entropic term plays an important role during the formation of the reactant complex when we move from a bimolecular to a unimolecular scenario (although, as we have previously explained, the role of entropy in our calculations could be overestimated). Once the reactant complex is formed, the changes in entropy become residual.

*Kinetic behavior of the Diels–Alder cycloaddition reactions.* We have also determined the structures of the TS in the cycloaddition reactions for the 10 most thermodynamically favored additions of cyclopentadiene over La@$C_{2v}$-$C_{82}$ and for the four additions that involved 1,2,3,4,5-pentamethylcyclopentadiene. In all of these cases, we started from a symmetric structure for the TS search and the optimization process led us to an asynchronous (but still concerted) TS, as has been observed in previous studies.[43b,56a,b] These TSs were characterized by having one—and only one—imaginary frequency, whose validity was confirmed by a full optimization towards the reactant complex and the product. The starting geometry in these latter cases was chosen based on small distortions (forward and reverse) along the transition vector of the TS (the normal mode eigenvector that corresponded to the imaginary frequency). By doing so, we discarded a possible radical intermediate in the reaction pathway and checked that the TS directly connected the reactant complex and the product in a single step, at least at this level of theory. Moreover, to discard the existence of a competitive stepwise mechanism, we optimized a triradical intermediate ($S=3/2$) that contained only one of the two C−C bonds that formed in the attack of Cp on bond **o** (the most favorable addition). This intermediate exists but it is 7.8 kcal mol$^{-1}$ higher in energy than the TS of the concerted pathway and, therefore, the existence of a more favored stepwise mechanism with a triradical intermediate has been ruled out. A single-point energy calculation of this triradical intermediate structure, but now with $S=0.5$, is 4.3 kcal mol$^{-1}$ lower than the TS of the concerted pathway. However, the geometry optimization starting from this structure leads to the final product, thus indicating that the intermediate with $S=0.5$ does not exist. We think that these results provide enough evidence of the non-existence of a monoradical intermediate in the pathway from the reactants to the products. All of the results of the concerted mechanisms are presented in Table 3.

We center our discussion on the reaction barriers that were obtained relative to the separated Cp and La@$C_{2v}$-$C_{82}$ reactants. The obtained results point to somewhat different kinetic behavior compared to the thermodynamic behavior discussed above. The addition of Cp is kinetically favored for the attacks on bonds **11** and **o**, with Gibbs energy barriers of 19.5 kcal mol$^{-1}$ and 20.2 kcal mol$^{-1}$ (23.4 kcal mol$^{-1}$ and 23.6 kcal mol$^{-1}$ at the B3LYP-$D_2$ level), respectively. However, as we have seen, the DA reaction on bond **11** is clearly thermodynamically endergonic, with a Gibbs reaction energy of 13.5 kcal mol$^{-1}$ (10.0 kcal mol$^{-1}$) at the BLYP-$D_2$ (B3LYP-$D_2$) level of theory. Moreover, its retro-DA reaction Gibbs energy barrier is about the half of the direct DA reaction (see the retro-reaction parameters in Table 4). This result means that, although the product can be formed first, because its barrier is in direct competition with that found for bond **o**, the reaction reverts back to the reactants because they are thermodynamically more stable. On the contrary, the DA reaction of bond **o** is the one with the lowest Gibbs reaction energy (7.8 kcal mol$^{-1}$ and 3.1 kcal mol$^{-1}$ at BLYP-$D_2$ and B3LYP-$D_2$ levels of theory, respectively). Furthermore, whereas the results at the B3LYP-$D_2$ level, which provides our most accurate theoretical data, show good agreement between the theoretical retro-DA barrier for attack on the **o** bond and the experimental barrier (see below), that is, the theoretical retro-DA barrier for attack on the bond **11** is 9.4 kcal mol$^{-1}$ smaller than the experimental value. Thus, by taking into account both the kinetic and the thermodynamic theoretical data, as well as the comparison between the DFT and experimental barriers, together with the fact that entropies are likely to be overestimated by using our approach, we conclude that only the cycloaddition to bond **o** can produce the final regioisomeric product of the reaction.

  

Table 3. BLYP-$D_2$/TZP//BLYP-$D_2$/DZP reaction barriers ($\Delta E^{\neq}$) and Gibbs reaction energy, enthalpy, and entropy barriers ($\Delta G^{\neq}$, $\Delta H^{\neq}$, and $\Delta S^{\neq}$) for the Diels–Alder cycloaddition reactions of cyclopentadiene and 1,2,3,4,5-pentamethylcyclopentadiene at the most favorable addition sites of the La@$C_{2v}$-$C_{82}$ EMF at 298.15 K. Bond lengths of the C–C bonds on which the reactions took place ($R_{full}$ (TS)) and of the two newly formed C–C bonds ($R_{CC}$ (TS)) in the transition-state structures are also presented.[a]

| Product | Bond type | $\Delta E^{\neq}$ [kcal mol$^{-1}$] | $\Delta G^{\neq}$ [kcal mol$^{-1}$] | $\Delta H^{\neq}$ [kcal mol$^{-1}$] | $\Delta S^{\neq}$ [cal K$^{-1}$ mol$^{-1}$] | $R_{full}$ (TS) [Å] | $R_{CC}$ (TS) [Å] | |
|---|---|---|---|---|---|---|---|---|
| *La@$C_{2v}$-$C_{82}$Cp* | | | | | | | | |
| **11** | B [6,6] | 4.8 | 19.5 | 5.6 | −46.7 | 1.495 | 1.886 | 2.856 |
| | | *11.0* | *11.8* | *11.6* | *−0.7* | | | |
| **12** | A [6,6] | 6.9 | 22.1 | 8.0 | −47.2 | 1.444 | 1.932 | 2.364 |
| | | *12.9* | *12.6* | *14.2* | *5.5* | | | |
| **16** | A [6,6] | 7.5 | 22.6 | 8.6 | −47.1 | 1.440 | 2.122 | 2.122 |
| | | *13.4* | *13.3* | *14.9* | *5.3* | | | |
| **19** | B [6,6] | 8.7 | 23.7 | 9.6 | −47.4 | 1.512 | 1.887 | 2.384 |
| | | *15.7* | *18.2* | *15.8* | *−8.0* | | | |
| **d** | C [5,6] | 10.2 | 24.1 | 10.8 | −44.3 | 1.518 | 1.867 | 2.489 |
| | | *16.7* | *16.5* | *17.1* | *2.1* | | | |
| **e** | C [5,6] | 9.6 | 23.5 | 10.3 | −44.3 | 1.495 | 1.861 | 2.763 |
| | | *16.1* | *17.6* | *15.9* | *−5.6* | | | |
| **f** | C [5,6] | 8.8 | 23.6 | 9.6 | −46.7 | 1.506 | 1.872 | 2.565 |
| | | *14.4* | *14.1* | *15.5* | *4.8* | | | |
| **h** | C [5,6] | 9.9 | 24.5 | 10.7 | −46.3 | 1.502 | 1.899 | 2.460 |
| | | *16.0* | *15.7* | *17.2* | *4.9* | | | |
| **j** | C [5,6] | 8.6 | 22.7 | 9.5 | −44.5 | 1.498 | 1.958 | 2.364 |
| | | *14.0* | *13.5* | *15.3* | *5.8* | | | |
| **o** | C [5,6] | 5.6 | 20.2 | 6.4 | −46.2 | 1.485 | 1.938 | 2.783 |
| | | *11.3* | *10.9* | *12.5* | *5.5* | | | |
| *La@$C_{2v}$-$C_{82}$Cp** | | | | | | | | |
| **11** | B [6,6] | −5.3 | 10.1 | −4.6 | −49.6 | 1.498 | 1.945 | 2.640 |
| | | *9.6* | *11.8* | *8.8* | *−10.1* | | | |
| **16** | A [6,6] | −3.7 | 10.3 | −3.2 | −45.1 | 1.445 | 2.131 | 2.132 |
| | | *10.3* | *11.4* | *9.5* | *−6.5* | | | |
| **j** | C [5,6] | −1.9 | 13.1 | −2.0 | −50.8 | 1.499 | 2.143 | 2.146 |
| | | *12.0* | *13.9* | *10.4* | *−11.5* | | | |
| **o** | C [5,6] | −5.4 | 9.5 | −4.8 | −48.1 | 1.487 | 2.026 | 2.563 |
| | | *8.9* | *10.8* | *8.2* | *−8.8* | | | |

[a] Values in italics were obtained relative to the first reactant complex that was formed.

The additions on bonds **o**, **12**, **16**, and **j**, which are the most favorable from a thermodynamic point of view, also have the lowest reaction barriers if we do not consider bond **11**. As noted above, the most kinetically favored attack of those four reactions is the attack on bond **o**, followed sequentially by the additions on bonds **12**, **16**, and **j**. By analyzing the Gibbs barriers, we found very similar entropic reaction barriers from the infinitely separated reactants for the different addition reactions (within the range −44.3 to −47.4 cal K$^{-1}$ mol$^{-1}$); thus, the enthalpy terms determine the lowest barrier height.

Higher Gibbs reaction barriers are found for [5,6] bonds **h**, **e**, and **d** and for [6,6] bond **19**. Thus, the kinetic results also exclude product **19** from being the main adduct that is formed from the attack of Cp onto La@$C_{2v}$-$C_{82}$. Bonds **h**, **e**, **d**, and **19**, were also the less-favored bonds from a thermodynamic point of view among the 10 selected. So, although the ordering of the reactivities from the kinetic and thermodynamic points of view is not exactly the same, there is a good correlation between them.[56c] Moreover, both parameters discard the possibility of bond **19** as being the most susceptible bond to cycloaddition.

Focusing on the addition of 1,2,3,4,5-pentamethylcyclopentadiene onto the La@$C_{2v}$-$C_{82}$ EMF, the results listed in Table 3 show that the most favorable addition from a kinetic point of view on the selected bonds is the attack on bond **o**. These results, together with the thermodynamic data, are in accordance with the experimental observations. The $\Delta E^{\neq}$ (int.) values for bonds **o**, **j**, **16**, and **11** are 2.4, 2.0, 3.1, and 1.4 kcal mol$^{-1}$, respectively, lower than the analogous values for the addition of Cp. Moreover, if we compare the Gibbs energy barriers, we find the same behavior (for example, a difference of 0.1 kcal mol$^{-1}$ for the addition on bond **o**). Bond **11** does not correspond to the attack with the lowest energy barrier, as in the Cp case, although its barrier is low; but bond **11** cannot be the major product of the DA addition because of the high endothermicity of the process and the low retro-reaction barrier.

The results shown in Table S1 and Figure S2 in the Supporting Information indicate that although the B3LYP-$D_2$ barriers are somewhat higher and the reaction energies are more exothermic than those obtained with the BLYP-$D_2$ functional, the trends remain basically the same and, therefore, the conclusions that are drawn at the BLYP-$D_2$ level still hold.

Our computational analysis and comparison between the DA reactions of Cp and Cp* show us that the reactivity and regioselectivity of both reactions starting from their respective initial reactant complexes are quite similar. Therefore, once the reactant complex is formed, the electronic effects of the methyl substituent groups are practically negligible in the last step of the reactions. This conclusion leads us to characterize the major product for the cycloaddition of Cp on the La@$C_{2v}$-$C_{82}$ EMF as the addition on bond **o**, the same regioselectivity found for the addition of Cp*, rather than on bonds **j**, **11**, **12**, or bond **19**, as suggested in a previous study.[23] At this point, we want to remind the reader that, because of the fast retro-DA reaction, the La@$C_{2v}$-$C_{82}$Cp product could not be characterized experimentally. Taken as a whole, our results indicate that attack on corannulene-type [5,6] bond **o**, which is far from the metal center, is the most favored for both Cp and Cp* if one takes into account the thermodynamics and kinetics of these DA cycloaddition reactions. This result agrees with the regioselectivity that

  

Table 4. BLYP-$D_2$/TZP//BLYP-$D_2$/DZP thermodynamic reaction parameters for the Diels–Alder cycloaddition reactions of cyclopentadiene and 1,2,3,4,5-pentamethylcyclopentadiene at the most favorable addition sites of the La@$C_{2v}$-$C_{82}$ EMF at 298.15 K. Values for the retro reactions ($\Delta G^{\neq}$ (retro), $\Delta H^{\neq}$ (retro), and $\Delta S^{\neq}$ (retro)) are also presented.[a]

| Product | Bond type | $\Delta E_R$ (retro) [kcal mol$^{-1}$] | $\Delta G_R$ (retro) [kcal mol$^{-1}$] | $\Delta H_R$ (retro) [kcal mol$^{-1}$] | $\Delta S_R$ (retro) [cal K$^{-1}$ mol$^{-1}$] | $\Delta E^{\neq}$ (retro) [kcal mol$^{-1}$] | $\Delta G^{\neq}$ (retro) [kcal mol$^{-1}$] | $\Delta H^{\neq}$ (retro) [kcal mol$^{-1}$] | $\Delta S^{\neq}$ (retro) [cal K$^{-1}$ mol$^{-1}$] |
|---|---|---|---|---|---|---|---|---|---|
| *La@$C_{2v}$-$C_{82}$Cp* | | | | | | | | | |
| **11** | B | 4.6 | −13.5 | 2.0 | 51.9 | 9.4 | 6.1 | 7.6 | 5.2 |
| | [6,6] | *−1.6* | *−5.7* | *−4.0* | *5.9* | | | | |
| **12** | A | 5.5 | −12.6 | 2.8 | 51.5 | 12.4 | 10.8 | 12.2 | 4.5 |
| | [6,6] | *−0.5* | *−3.1* | *−3.5* | *−1.2* | | | | |
| **16** | A | 6.4 | −11.8 | 3.6 | 51.6 | 13.9 | 11.0 | 12.1 | 3.6 |
| | [6,6] | *0.5* | *−2.5* | *−2.7* | *−0.7* | | | | |
| **19** | B | 5.1 | −12.7 | 2.5 | 51.0 | 13.8 | 12.4 | 14.5 | 7.0 |
| | [6,6] | *−1.9* | *−7.1* | *−3.7* | *11.7* | | | | |
| **d** | C | 6.2 | −11.7 | 3.6 | 51.3 | 16.4 | 10.3 | 12.5 | 7.6 |
| | [5,6] | *−0.3* | *−4.1* | *−2.7* | *4.9* | | | | |
| **e** | C | 4.9 | −13.2 | 2.3 | 51.9 | 14.5 | 10.7 | 12.3 | 5.5 |
| | [5,6] | *−1.6* | *−7.3* | *−3.4* | *13.1* | | | | |
| **f** | C | 5.3 | −12.9 | 2.7 | 52.2 | 14.1 | 10.8 | 12.2 | 4.7 |
| | [5,6] | *−0.2* | *−3.4* | *−3.2* | *0.7* | | | | |
| **h** | C | 4.0 | −13.7 | 1.5 | 50.9 | 13.9 | 11.8 | 13.9 | 6.9 |
| | [5,6] | *−2.0* | *−4.9* | *−5.0* | *−0.3* | | | | |
| **j** | C | 7.1 | −10.9 | 4.4 | 51.5 | 15.7 | 12.4 | 14.0 | 5.5 |
| | [5,6] | *1.7* | *−1.7* | *−1.4* | *1.1* | | | | |
| **o** | C | 10.5 | −7.8 | 7.6 | 51.8 | 16.0 | 12.4 | 14.0 | 5.5 |
| | [5,6] | *4.7* | *1.5* | *1.5* | *0.1* | | | | |
| *La@$C_{2v}$-$C_{82}$Cp** | | | | | | | | | |
| **11** | B | 13.1 | −5.6 | 11.1 | 56.2 | 7.8 | 10.2 | 12.6 | 7.8 |
| | [6,6] | *−1.8* | *−7.3* | *−2.3* | *16.7* | | | | |
| **16** | A | 14.8 | −4.0 | 12.8 | 56.3 | 11.1 | 6.3 | 9.6 | 11.2 |
| | [6,6] | 0.8 | *−5.1* | *0.1* | *17.7* | | | | |
| **j** | C | 15.5 | −2.9 | 13.6 | 55.3 | 13.6 | 10.2 | 11.6 | 4.5 |
| | [5,6] | *1.7* | *−3.6* | *1.1* | *15.9* | | | | |
| **o** | C | 19.4 | 0.7 | 17.4 | 55.9 | 14.0 | 10.2 | 12.6 | 7.8 |
| | [5,6] | *5.1* | *−0.5* | *4.4* | *16.6* | | | | |

[a] Values in italics were obtained relative to the first reactant complex that was formed.

was observed in a recent Prato cycloaddition of azomethine ylide to La@$C_{2v}$-$C_{82}$.[32] Moreover, this result is similar to that found for $Ti_2C_2$@$D_{3h}$-$C_{78}$, where corannulene-type [5,6] bonds **c** and **f** where found to be among the most reactive.[43b]

**Understanding the different stabilities of the products and the reversibility of the reaction. The key role of the reactant complex**: The experimental kinetic parameters for the retro-DA reaction of the La@$C_{2v}$-$C_{82}$Cp adduct were determined by Maeda et al.[23] These authors found an activation energy ($E_a$) of 23.9 kcal mol$^{-1}$, $\Delta G^{\neq}$ = 22.9 kcal mol$^{-1}$, $\Delta H^{\neq}$ = 23.4 kcal mol$^{-1}$, and $\Delta S^{\neq}$ = 1.7 cal K$^{-1}$ mol$^{-1}$. Herein, we have effectively characterized the product that was obtained from the DA reaction between La@$C_{2v}$-$C_{82}$ and Cp to be product **o**. Thus, we can study the retro-reaction by correctly considering the major product that is formed during the direct DA cycloaddition reaction. Our thermodynamic results at the BLYP-$D_2$/TZP//BLYP-$D_2$/DZP level of theory for the retro-DA reaction of product **o** (Table 4) are lower than those found experimentally (the differences are 10.5 and 9.4 kcal mol$^{-1}$ for $\Delta G^{\neq}$ and $\Delta H^{\neq}$, respectively, and 3.8 cal mol$^{-1}$ K$^{-1}$ for $\Delta S^{\neq}$). As mentioned in the Computational Details, it is known that BLYP underestimates the DA barriers, whilst B3LYP-$D_2$ provides better estimates of the DA barriers in fullerenes.[43a] Our results for the retro-DA reaction at the B3LYP-$D_2$/TZP//BLYP-$D_2$/DZP level of theory, that is, $\Delta G^{\neq}$ = 20.5 (2.4) kcal mol$^{-1}$, $\Delta H^{\neq}$ = 22.2 (1.2) kcal mol$^{-1}$, and $\Delta S^{\neq}$ = 5.5 (−3.8) cal K$^{-1}$ mol$^{-1}$ (differences with respect to the experimental values are given in parentheses), confirm this point. As the small observed differences show, the experimental values for the retro-DA reaction of La@$C_{82}$Cp are reasonably well-reproduced by the B3LYP-$D_2$ functional. It is worth noting that, as shown above, the trends that are derived by using the BLYP-$D_2$ and B3LYP-$D_2$ functionals are basically the same.

Once the intermediate is formed, both of the DA cycloaddition reactions of Cp and Cp* show similar thermodynamics and kinetics (Figure 4 and the Supporting Information, Table S2). Thus, the retro-reaction barriers for both **o** adducts are very similar, with the Gibbs energy barrier of the Cp* adduct being only 1.5 kcal mol$^{-1}$ lower than that of the Cp adduct at the B3LYP-$D_2$/TZP//BLYP-$D_2$/DZP level of theory (2.2 kcal mol$^{-1}$ at the BLYP-$D_2$/TZP//BLYP-$D_2$/DZP level of theory). The Gibbs energy profile for the additions of Cp and Cp* on bond **o** from a retro-DA point of view are represented in Figure 4. However, as mentioned above, the relative experimental stability of La@$C_{2v}$-$C_{82}$Cp* is consider-

  

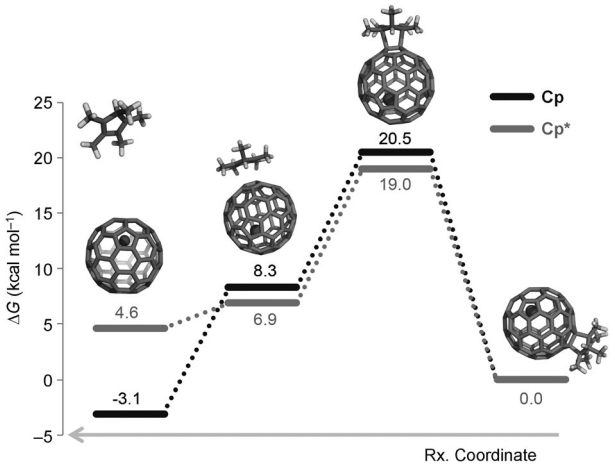


Figure 4. Gibbs energy profile obtained at the B3LYP-$D_2$/TZP//BLYP-$D_2$/DZP level of theory of the Diels–Alder cycloadditions between La@$C_{2v}$-$C_{82}$ and Cp (black) or Cp* (gray) for attack on the most reactive [5,6] bond (bond **o**). Relative Gibbs energy values are given in kcal mol$^{-1}$.

ably greater than that of La@$C_{2v}$-$C_{82}$Cp, although its DFT-calculated retro-reaction barrier is 2 kcal mol$^{-1}$ lower. Thus, the question is where do the significant differences between the stabilities and lifetimes of both products come from?

The answer is provided by the key role of the reactant complex. As shown in Figure 4, from a retro-reaction point of view, the stability of the initial complex is practically the same (difference of 1.4 kcal mol$^{-1}$). Moreover, by taking into account the barrier heights, one could expect that the Cp* product is the less stable in an opposite manner to what is found experimentally. However, by focusing on the stabilities of the intermediate reactant complexes with respect to the diene and the dienophile at infinite separation, we found different behaviors (Figure 4 and the Supporting Information, Table S2). Because we have shown above that the B3LYP-$D_2$ level better represents the absolute energy values, we will use these energies in Figure 4 and in the following discussion. The Gibbs energy of formation for the reactant complex of Cp* and La@$C_{2v}$-$C_{82}$ is slightly positive (2.3 kcal mol$^{-1}$, at the B3LYP-$D_2$ level), whereas, for the Cp intermediate, we observe a large positive value (11.4 kcal mol$^{-1}$), which clearly indicates a preference for dissociation of the reactant complex. This difference arises from the enthalpic contributions, in which the enthalpy of formation of the Cp* reactant complex (−9.4 kcal mol$^{-1}$) is more than the double that of the Cp complex (−3.9 kcal mol$^{-1}$), which, in turn, is the result of the higher long-range dispersion interactions in the Cp* case.

Then, for the retro reaction, with Cp, once the reactant complex is formed, the system rapidly dissociates to yield the separated reactants. The retro-cycloaddition reaction is also possible for the Cp* product. However, in this case, the reactant complex that is formed has a low direct DA barrier (lower than the corresponding retro-DA barrier). Thus, the Cp* reactant complex can react again to give the DA adduct. If, as pointed out in the literature,[57] the entropy change between the reactants at infinite distance and the reactant complex in solution is lower than the gas-phase DFT value, the Cp* reactant complex could even be stable, or at least dissociate slowly. Summing up, for the La@$C_{2v}$-$C_{82}$Cp* system, a dynamic equilibrium between the DA adduct and the reactant complex is established because the direct and retro reactions can compete with one another. This equilibrium leads to longer half-life decomposition times for the Cp* system than for the Cp system, as was observed experimentally.

Finally, we analyzed the effect of the dispersion-energy contributions on the studied reaction pathways. Figure 5 shows the reaction-energy profiles for the Cp and Cp* reactions from a retro-DA reaction point of view (see the Supporting Information, Table S3). A lack of dispersion corrections completely changes the reaction-energy profiles and results in endothermic DA cycloadditions, as well as the loss of the reactant complex. Interestingly, the energy profiles relative to the reactant complex of the Cp and Cp* additions are quite similar. This result indicates that the electronic effects of the methyl substituents do not play a major role in explaining the different half-life decomposition times

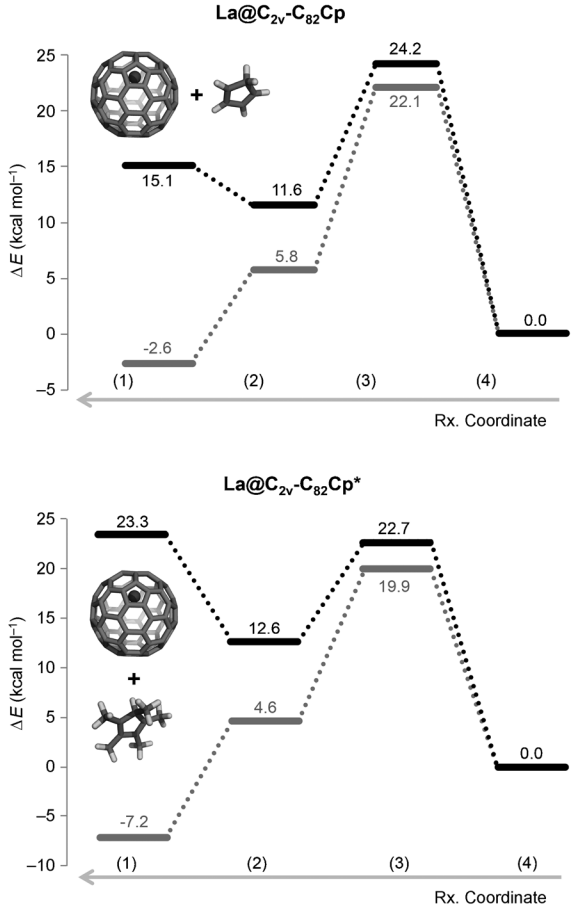


Figure 5. Energy profiles at the B3LYP-$D_2$/TZP//BLYP-$D_2$/DZP level of theory of the Diels–Alder cycloadditions between La@$C_{2v}$-$C_{82}$ and a) Cp and b) Cp* for attack on the most reactive [5,6] bond (bond **o**) of La@$C_{2v}$-$C_{82}$ when dispersion effects were including (black) and not included (gray). The stationary points represented are: (1) reactants, (2) reactant intermediate structure, (3) transition state, and (4) product. Relative energy values are given in kcal mol$^{-1}$.

  

of Cp and Cp*. In fact, the electronic effects of the Cp* group lower the barrier of the retro-DA and should favor the dissociation of La@$C_{82}$Cp*. Thus, the higher stability of the La@$C_{82}$Cp* adduct, which is ascribed to the electronic effects of the methyl groups on the Cp ring,[30] has to be attributed instead to long-range stabilizing dispersion interactions. Without considering them, as shown in Figure 5, the Cp monoadduct would be the one most stable, with a higher retro-barrier and practically thermoneutral reaction energy, in contrast to the lower barrier and large exothermic retro-reaction energy found for the Cp* system. When dispersion interactions are considered, this situation is inverted, as discussed above. This result confirms that dispersion corrections are essential for analyzing the reactivity of fullerenes, nanotubes, and graphene sheets.[43]

## Conclusion

We have performed BLYP-$D_2$/TZP//BLYP-$D_2$/DZP and B3LYP-$D_2$/TZP//BLYP-$D_2$/DZP calculations of the DA cycloaddition reactions of cyclopentadiene (Cp) and 1,2,3,4,5-pentamethylcyclopentadiene (Cp*) with different bonds of La@$C_{2v}$-$C_{82}$. Experimentally, the attack of Cp was proposed to occur on bond **19**, whereas that of Cp* was confirmed by X-ray analysis to be on bond **o**. Our results clearly show that, in both DA cycloadditions, the preferred attack is on bond **o**, both thermodynamically and kinetically. Only in the case of Cp does bond **11** have a lower barrier for the DA than bond **o**. However, the attack on bond **11** is very endergonic and, consequently, once the product is formed it reverts back to the original reactants. Thus, our results correct the previous wrong assignment for the regioselectivity of Cp attack, which was based only on the shape of the SOMO of La@$C_{2v}$-$C_{82}$, and show that the major adducts of the DA cycloadditions of both Cp and Cp* to La@$C_{2v}$-$C_{82}$ are the result of attack on bond **o**.

Furthermore, it was found experimentally that the stabilities of the Cp and Cp* adducts were significantly different, that is, the decomposition of La@$C_{2v}$-$C_{82}$Cp was one order of magnitude faster than that of La@$C_{2v}$-$C_{82}$Cp*. Our results indicate that the electronic effects of the methyl substituents do not play a major role in explaining the different half-life decomposition times of Cp and Cp*, as previously suggested.[30] In fact, the electronic effects of the methyl groups in Cp* lower the barrier of the retro-DA and, hence, should favor the dissociation of La@$C_{82}$Cp*. We show that the higher stability of the La@$C_{82}$Cp* adduct is due to the long-range stabilizing dispersion interactions, which are about 9 kcal mol$^{-1}$ higher in terms of Gibbs energy in the reactant complex with Cp* compared to that with Cp. In the retro-DA process, once the reactant complex is formed, the large stabilization of the Cp* and La@$C_{2v}$-$C_{82}$ reactant complex makes the DA cycloaddition compete with the retro-DA reaction and explains the higher stability of the La@$C_{2v}$-$C_{82}$Cp* adduct.

## Acknowledgements

The following organizations are thanked for financial support: the Ministerio de Ciencia e Innovación (MICINN, project numbers CTQ2011-23156/BQU and CTQ2011-25086/BQU), the Generalitat de Catalunya (project numbers 2009SGR637 and 2009SGR528 and Xarxa de Referència en Química Teòrica i Computacional), and the FEDER fund (European Fund for Regional Development, grant number UNGI08-4E-003). M.G.-B. thanks the Spanish MEC for a doctoral fellowship (number AP2010-2517). The authors are also grateful for the computer resources, technical expertise, and assistance provided by the Barcelona Supercomputing Center (Centro Nacional de Supercomputación). Support of the research of M.S. was received through the ICREA Academia 2009 prize for excellence in research, funded by the DIUE of the Generalitat de Catalunya. Excellent service by the Centre de Serveis Científics i Acadèmics de Catalunya (CESCA) is gratefully acknowledged.

[1] J. R. Heath, S. C. O'Brien, Q. Zhang, Y. Liu, R. F. Curl, H. W. Kroto, F. K. Tittel, R. E. Smalley, *J. Am. Chem. Soc.* **1985**, *107*, 7779–7780.
[2] a) M. Yamada, T. Akasaka, S. Nagase, *Acc. Chem. Res.* **2010**, *43*, 92–102; b) *Endofullerenes: A New Family of Carbon Cluster*, Akasaka, T.; Nagase, S. eds., Kluwer, Dordrecht, **2002**; c) H. Hu, W.-D. Cheng, S.-H. Huang, Z. Xie, H. Zhang, *J. Theor. Comput. Chem.* **2008**, *7*, 737–749.
[3] Y. Chai, T. Guo, C. Jin, R. E. Haufler, L. P. F. Chibante, J. Fure, L. Wang, J. M. Alford, R. E. Smalley, *J. Phys. Chem.* **1991**, *95*, 7564–7568.
[4] a) M. N. Chaur, F. Melin, A. L. Ortiz, L. Echegoyen, *Angew. Chem.* **2009**, *121*, 7650–7675; *Angew. Chem. Int. Ed.* **2009**, *48*, 7514–7538; b) S. Liu, S. Sun, *J. Organomet. Chem.* **2000**, *599*, 74–86.
[5] Y. Takano, A. Yomogida, H. Nikawa, M. Yamada, T. Wakahara, T. Tsuchiya, M. O. Ishitsuka, Y. Maeda, T. Akasaka, T. Kato, Z. Slanina, N. Mizorogi, S. Nagase, *J. Am. Chem. Soc.* **2008**, *130*, 16224–16230.
[6] T. Akasaka, T. Wakahara, S. Nagase, K. Kobayashi, M. Waelchli, K. Yamamoto, M. Kondo, S. Shirakura, Y. Maeda, T. Kato, M. Kako, Y. Nakadaira, X. Gao, E. V. Caemelbecke, K. M. Kadish, *J. Phys. Chem. B* **2001**, *105*, 2971–2974.
[7] X. Lu, K. Nakajima, Y. Iiduka, H. Nikawa, N. Mizorogi, Z. Slanina, T. Tsuchiya, S. Nagase, T. Akasaka, *J. Am. Chem. Soc.* **2011**, *133*, 19553–19558.
[8] a) T. Inoue, T. Tomiyama, T. Sugai, T. Okazaki, T. Suematsu, N. Fujii, H. Utsumi, K. Nojima, H. Shinohara, *J. Phys. Chem. B* **2004**, *108*, 7573–7579; b) T. Inoue, T. Tomiyama, T. Sugai, H. Shinohara, *Chem. Phys. Lett.* **2003**, *382*, 226–231; c) E. Nishibori, M. Ishihara, M. Takata, M. Sakata, Y. Ito, T. Inoue, H. Shinohara, *Chem. Phys. Lett.* **2006**, *433*, 120–124.
[9] B. Q. Mercado, N. Chen, A. Rodríguez-Fortea, M. A. Mackey, S. Stevenson, L. Echegoyen, J. M. Poblet, M. M. Olmstead, A. L. Balch, *J. Am. Chem. Soc.* **2011**, *133*, 6752–6760.
[10] B. Q. Mercado, M. A. Stuart, M. A. Mackey, J. E. Pickens, B. S. Confait, S. Stevenson, M. L. Easterling, R. Valencia, A. Rodríguez-Fortea, J. M. Poblet, M. M. Olmstead, A. L. Balch, *J. Am. Chem. Soc.* **2010**, *132*, 12098–12105.
[11] a) M. Takata, B. Umeda, E. Nishibori, M. Sakata, Y. Saitot, M. Ohno, H. Shinohara, *Nature* **1995**, *377*, 46–49; b) E. Y. Misochko, A. V. Akimov, V. A. Belov, D. A. Tyurin, V. P. Bubnov, I. E. Kareev, E. B. Yagubskii, *Phys. Chem. Chem. Phys.* **2010**, *12*, 8863–8869.
[12] E. Nishibori, M. Takata, M. Sakata, M. Inakuma, H. Shinohara, *Chem. Phys. Lett.* **1998**, *298*, 79–84.
[13] a) K. Muthukumar, J. A. Larsson, *J. Phys. Chem. A* **2008**, *112*, 1071–1075; b) M. Yamada, T. Wakahara, Y. Lian, T. Tsuchiya, T. Akasaka, M. Waelchli, N. Mizorogi, S. Nagase, K. M. Kadish, *J. Am. Chem. Soc.* **2006**, *128*, 1400–1401.
[14] H. Kurihara, X. Lu, Y. Iiduka, N. Mizorogi, Z. Slanina, T. Tsuchiya, S. Nagase, T. Akasaka, *Chem. Commun.* **2012**, *48*, 1290–1292.

  

[15] a) N. Tagmatarchis, H. Shinohara, *Chem. Mater.* **2000**, *12*, 3222–3226; b) Y. Iiduka, T. Wakahara, K. Nakajima, T. Nakahodo, T. Tsuchiya, Y. Maeda, T. Akasaka, K. Yoza, M. T. H. Liu, N. Mizorogi, S. Nagase, *Angew. Chem.* **2007**, *119*, 5658–5660; *Angew. Chem. Int. Ed.* **2007**, *46*, 5562–5564; c) Y. Iiduka, T. Wakahara, K. Nakajima, T. Tsuchiya, T. Nakahodo, Y. Maeda, T. Akasaka, N. Mizorogi, S. Nagase, *Chem. Commun.* **2006**, 2057–2059; d) Y. Yamazaki, K. Nakajima, T. Wakahara, T. Tsuchiya, M. O. Ishitsuka, Y. Maeda, T. Akasaka, M. Waelchli, N. Mizorogi, S. Nagase, *Angew. Chem.* **2008**, *120*, 8023–8026; *Angew. Chem. Int. Ed.* **2008**, *47*, 7905–7908.

[16] L. Dunsch, S. Yang, L. Zhang, A. Svitova, S. Oswald, A. A. Popov, *J. Am. Chem. Soc.* **2010**, *132*, 5413–5421.

[17] E. Nishibori, M. Takata, M. Sakata, H. Tanaka, M. Hasegawa, H. Shinohara, *Chem. Phys. Lett.* **2000**, *330*, 497–502.

[18] P. Jin, C. Hao, S. Li, W. Mi, Z. Sun, J. Zhang, Q. Hou, *J. Phys. Chem. A* **2007**, *111*, 167–169.

[19] a) S. Nagase, K. Kobayashi, *Chem. Phys. Lett.* **1993**, *214*, 57–63; b) T. Akasaka, T. Kato, K. Kobayashi, S. Nagase, K. Yamamoto, H. Funasaka, T. Takahashi, *Nature* **1995**, *374*, 600–601; c) R. Valencia, A. Rodríguez-Fortea, J. M. Poblet, *J. Phys. Chem. A* **2008**, *112*, 4550–4555.

[20] Y. Matsunaga, Y. Maeda, T. Wakahara, T. Tsuchiya, M. O. Ishitsuka, T. Akasaka, N. Mizorogi, K. Kobayashi, S. Nagase, K. M. Kadish, *ITE Lett.* **2006**, *7*, 43–49.

[21] T. Akasaka, T. Wakahara, S. Nagase, K. Kobayashi, M. Waelchli, K. Yamamoto, M. Kondo, S. Shirakura, S. Okubo, Y. Maeda, T. Kato, M. Kako, Y. Nakadaira, R. Nagahata, X. Gao, E. Van Caemelbecke, K. M. Kadish, *J. Am. Chem. Soc.* **2000**, *122*, 9316–9317.

[22] Y. Maeda, J. Miyashita, T. Hasegawa, T. Wakahara, T. Tsuchiya, L. Feng, Y. Lian, T. Akasaka, K. Kobayashi, S. Nagase, M. Kako, K. Yamamoto, K. M. Kadish, *J. Am. Chem. Soc.* **2005**, *127*, 2143–2146.

[23] Y. Maeda, J. Miyashita, T. Hasegawa, T. Wakahara, T. Tsuchiya, T. Nakahodo, T. Akasaka, N. Mizorogi, K. Kobayashi, S. Nagase, T. Kato, N. Ban, H. Nakajima, Y. Watanabe, *J. Am. Chem. Soc.* **2005**, *127*, 12190–12191.

[24] T. Akasaka, T. Kato, S. Nagase, K. Kobayashi, K. Yamamoto, H. Funasaka, T. Takahashi, *Tetrahedron* **1996**, *52*, 5015–5020.

[25] a) L. Feng, T. Nakahodo, T. Wakahara, T. Tsuchiya, Y. Maeda, T. Akasaka, T. Kato, E. Horn, K. Yoza, N. Mizorogi, S. Nagase, *J. Am. Chem. Soc.* **2005**, *127*, 17136–17137; b) L. Feng, T. Tsuchiya, T. Wakahara, T. Nakahodo, Q. Piao, Y. Maeda, T. Akasaka, T. Kato, K. Yoza, E. Horn, N. Mizorogi, S. Nagase, *J. Am. Chem. Soc.* **2006**, *128*, 5990–5991; c) L. Feng, T. Wakahara, T. Nakahodo, T. Tsuchiya, Q. Piao, Y. Maeda, Y. Lian, T. Akasaka, E. Horn, K. Yoza, T. Kato, N. Mizorogi, S. Nagase, *Chem. Eur. J.* **2006**, *12*, 5578–5586.

[26] T. Suzuki, Y. Maruyama, T. Kato, T. Akasaka, K. Kobayashi, S. Nagase, K. Yamamoto, H. Funasaka, T. Takahashi, *J. Am. Chem. Soc.* **1995**, *117*, 9606–9607.

[27] L. Feng, Z. Slanina, S. Sato, K. Yoza, T. Tsuchiya, N. Mizorogi, T. Akasaka, S. Nagase, N. Martín, D. M. Guldi, *Angew. Chem.* **2011**, *123*, 6031–6034; *Angew. Chem. Int. Ed.* **2011**, *50*, 5909–5912.

[28] Y. Maeda, Y. Matsunaga, T. Wakahara, S. Takahashi, T. Tsuchiya, M. O. Ishitsuka, T. Hasegawa, T. Akasaka, M. T. H. Liu, K. Kokura, E. Horn, K. Yoza, T. Kato, S. Okubo, K. Kobayashi, S. Nagase, K. Yamamoto, *J. Am. Chem. Soc.* **2004**, *126*, 6858–6859.

[29] M. Hachiya, H. Nikawa, N. Mizorogi, T. Tsuchiya, X. Lu, T. Akasaka, *J. Am. Chem. Soc.* **2012**, *134*, 15550–15555.

[30] Y. Maeda, S. Sato, K. Inada, H. Nikawa, M. Yamada, N. Mizorogi, T. Hasegawa, T. Tsuchiya, T. Akasaka, T. Kato, Z. Slanina, S. Nagase, *Chem. Eur. J.* **2010**, *16*, 2193–2197.

[31] Y. Takano, M. O. Ishitsuka, T. Tsuchiya, T. Akasaka, T. Kato, S. Nagase, *Chem. Commun.* **2010**, *46*, 8035–8036.

[32] Y. Takano, S. Obuchi, N. Mizorogi, R. García, M. Á. Herranz, M. Rudolf, S. Wolfrum, D. M. Guldi, N. Martín, S. Nagase, T. Akasaka, *J. Am. Chem. Soc.* **2012**, *134*, 16103–16106.

[33] A. Hirsch, M. Brettreich, *Fullerenes: Chemistry and Reactions*, Weinheim, **2004**.

[34] S. Osuna, M. Swart, M. Solà, *Phys. Chem. Chem. Phys.* **2011**, *13*, 3585–3603.

[35] ADF 2010.01, E. J. Baerends, T. Ziegler, J. Autschbach, D. Bashford, A. Bérces, F. M. Bickelhaupt, C. Bo, P. M. Boerrigter, L. Cavallo, D. P. Chong, L. Deng, R. M. Dickson, D. E. Ellis, M. v. Faassen, L. Fan, T. H. Fischer, C. Fonseca Guerra, A. Ghysels, A. Giammona, S. J. A. van Gisbergen, A. W. Götz, J. A. Groeneveld, O. V. Gritsenko, M. Grüning, S. Gusarov, F. E. Harris, P. van den Hoek, C. R. Jacob, H. Jacobsen, L. Jensen, J. W. Kaminski, G. van Kessel, F. Kootstra, A. Kovalenko, M. V. Krykunov, E. van Lenthe, D. A. McCormack, A. Michalak, M. Mitoraj, J. Neugebauer, V. P. Nicu, L. Noodleman, V. P. Osinga, S. Patchkovskii, P. H. T. Philipsen, D. Post, C. C. Pye, W. Ravenek, J. I. Rodríguez, P. Ros, P. R. T. Schipper, G. Schreckenbach, J. S. Seldenthuis, M. Seth, J. G. Snijders, M. Solà, M. Swart, D. Swerhone, G. te Velde, P. Vernooijs, L. Versluis, L. Visscher, O. Visser, F. Wang, T. A. Wesolowski, E. M. van Wezenbeek, G. Wiesenekker, S. K. Wolff, T. K. Woo, A. L. Yakovlev, SCM, Amsterdam, **2010**.

[36] G. te Velde, F. M. Bickelhaupt, E. J. Baerends, C. Fonseca Guerra, S. J. A. van Gisbergen, J. G. Snijders, T. Ziegler, *J. Comput. Chem.* **2001**, *22*, 931–967.

[37] M. Swart, J. G. Snijders, *Theor. Chem. Acc.* **2003**, *110*, 34–41 (erratum: ibid. *111*, 56).

[38] E. van Lenthe, E. J. Baerends, J. G. Snijders, *J. Chem. Phys.* **1993**, *99*, 4597–4610.

[39] E. J. Baerends, D. E. Ellis, P. Ros, *Chem. Phys.* **1973**, *2*, 41–51.

[40] A. D. Becke, *Phys. Rev. A* **1988**, *38*, 3098–3100.

[41] C. Lee, W. Yang, R. G. Parr, *Phys. Rev. B* **1988**, *37*, 785–789.

[42] a) S. Grimme, *J. Comput. Chem.* **2006**, *27*, 1787–1799; b) S. Grimme, J. Antony, S. Ehrlich, H. Krieg, *J. Chem. Phys.* **2010**, *132*, 154104.

[43] a) S. Osuna, M. Swart, M. Solà, *J. Phys. Chem. A* **2011**, *115*, 3491–3496; b) M. Garcia-Borràs, S. Osuna, J. M. Luis, M. Swart, M. Solà, *Chem. Eur. J.* **2012**, *18*, 7141–7154.

[44] S. F. Boys, F. Bernardi, *Mol. Phys.* **1970**, *19*, 553–566.

[45] M. Swart, M. Solà, F. M. Bickelhaupt, *J. Comput. Chem.* **2007**, *28*, 1551–1560.

[46] S. Osuna, J. Morera, M. Cases, K. Morokuma, M. Solà, *J. Phys. Chem. A* **2009**, *113*, 9721–9726.

[47] a) A. D. Becke, *J. Chem. Phys.* **1993**, *98*, 5648–5652; b) P. J. Stephens, F. J. Devlin, C. F. Chabalowski, M. J. Frisch, *J. Phys. Chem.* **1994**, *98*, 11623–11627.

[48] M. Swart, F. M. Bickelhaupt, *J. Comput. Chem.* **2008**, *29*, 724–734.

[49] M. Swart, F. M. Bickelhaupt, *Int. J. Quantum Chem.* **2006**, *106*, 2536–2544.

[50] S. K. Wolff, *Int. J. Quantum Chem.* **2005**, *104*, 645–659.

[51] P. Atkins, J. De Paula, *Physical Chemistry*, Oxford University Press, Oxford, **2006**.

[52] a) R. C. Haddon, *J. Phys. Chem. A* **2001**, *105*, 4164–4165; b) R. C. Haddon, S. Y. Chow, *J. Am. Chem. Soc.* **1998**, *120*, 10494–10496.

[53] R. C. Haddon, QCPE 508/QCMP 044, *QCPE Bull.* **1988**, *8*.

[54] A. Rodríguez-Fortea, N. Alegret, A. L. Balch, J. M. Poblet, *Nat. Chem.* **2010**, *2*, 955–961.

[55] M. Solà, J. Mestres, M. Duran, *J. Phys. Chem.* **1995**, *99*, 10752–10758.

[56] a) S. Osuna, M. Swart, J. M. Campanera, J. M. Poblet, M. Solà, *J. Am. Chem. Soc.* **2008**, *130*, 6206–6214; b) S. Osuna, M. Swart, M. Solà, *J. Am. Chem. Soc.* **2009**, *131*, 129–139; c) M. Garcia-Borràs, A. Romero-Rivera, S. Osuna, J. M. Luis, M. Swart, M. Solà, *J. Chem. Theory Comput.* **2012**, *8*, 1671–1683.

[57] a) M. Strajbl, Y. Y. Sham, J. Villà, Z. T. Chu, A. Warshel, *J. Phys. Chem. B* **2000**, *104*, 4578–4584; b) Y. Liang, S. Liu, Y. Xia, Y. Li, Z.-X. Yu, *Chem. Eur. J.* **2008**, *14*, 4361–4373; c) Z.-X. Yu, K. N. Houk, *J. Am. Chem. Soc.* **2003**, *125*, 13825–13830.

Received: October 3, 2012
Revised: December 30, 2012
Published online: February 10, 2013

  